left. Equation (33) is solved for u and the eight matching equations are solved for the eight remaining constants. The self-consistent equations for A_0 and A_1 are solved as above, but now remembering that u is not of $O(q)$, but contains a component of $O(1)$. The coefficient c_j^R corresponding to the outgoing wave $e^{i|\gamma_R|z}$ is obtained by this procedure. It is the transmission coefficient. We obtain at the same time, of course, the reflection coefficient, the c_j^L which multiplies $e^{-i|\gamma_L|z}$.

VI. CONCLUSION

As long as the high-frequency expansion to the RPA is valid, we may obtain expressions for the dispersion of surface plasmons and the transmission and reflection coefficients of bulk plasmons in a bimetallic system, which depend only on average properties of the electron wave function. As the ratio of the electron densities in the two metals differs too much from 1, the modes of the system begin to couple to individual particle-hole excitations, whose density of states do not seem to be related in any simple way to these average features. Because of this "Landau damping" effect, then, it is difficult to extend our analysis of the plasma oscillations at a bimetallic interface to those of a metal-vacuum interface.

ACKNOWLEDGMENT

The author wishes to thank Professor C. B. Duke for encouraging him to undertake this investigation, and for many useful discussions.

*Work supported in part by the U. S. Army Research Office (Durham) under Contract No. DA-HC04-69-C-0007.

[1]C. Kunz, Z. Physik 196, 311 (1966).

[2]C. B. Duke, A. J. Howsmon, and G. E. Laramore, J. Vacuum Sci. Technol. 8, 5 (1971).

[3]P. J. Feibelman, Phys. Rev. B 3, 220 (1971).

[4]R. H. Ritchie, Progr. Theoret. Phys. (Kyoto) 29, 607 (1963); H. Kanazawa, *ibid.* 26, 851 (1961).

[5]P. A. Fedders, Phys. Rev. 153, 438 (1967); D. M. Newns, Phys. Rev. B 1, 3034 (1970).

[6]A. J. Bennett, Phys. Rev. B 1, 203 (1970).

[7]M. Gell-Mann and K. A. Brueckner, Phys. Rev. 106, 364 (1957).

[8]P. J. Feibelman, Phys. Rev. 176, 551 (1968), referred to in the text as I.

[9]J. Harris and A. Griffin (unpublished).

[10]We imagine the metal to be a semi-infinite flat slab of jellium.

[11]If $n_0(z) = n_\infty = \text{const}$ for $z < 0$, then the bulk plasmon $\varphi(z)$ is derived from Eq. (15) by imposing the condition

$$\int_0^\infty dz \, \frac{dn_0}{dz} \, \varphi(z) = 0.$$

[12]In bulk,

$$p_\perp \equiv \int_{k<k_F} \frac{d^3k}{(2\pi)^3} \frac{k_z^2}{m} = \frac{1}{3m} \frac{4\pi}{8\pi^3} \tfrac{1}{5} k_F^5 = \tfrac{1}{5} m v_F^2 n_\infty \ ,$$

with $n_\infty \equiv k_F^3/6\pi^2$.

[13]In an infinite system, the RPA energy denominator, $\omega - \omega_{k+qn} + \omega_{kn}$, becomes $\omega - v_F k \cos\theta - k^2/2m$, where k is the three-dimensional wave vector and $-\pi < \theta < \pi$. The high-frequency expansion is valid only if $\omega \gg |v_F k| + k^2/2m$. Thus, it is not valid if $k^2 \approx 2m\omega$. For such short wavelengths, Landau damping is important.

[14]See also Ref. 3, and J. W. Gadzuk, Phys. Rev. B 1, 1267 (1970).

[15]See Ref. 13.

[16]See, e.g., Ref. 3.

PHYSICAL REVIEW B VOLUME 3, NUMBER 9 1 MAY 1971

Exchange Corrections to Hot-Electron Lifetimes*

Leonard Kleinman
Department of Physics, University of Texas, Austin, Texas 78712
(Received 30 October 1970)

We obtain an improved approximation for the inverse vertex function $\epsilon_{\vec{k}t}(\vec{\kappa}, \omega)$ with exchange corrections. The imaginary part of the self-energy of hot electrons is calculated and compared with the random-phase-approximation (RPA) values. The RPA results differ significantly from Quinn's earlier RPA results owing to improved computational facilities. The mean free path of an electron 5 eV above the Fermi surface in aluminum is compared with Kanter's experimental value.

I. INTRODUCTION

Although exchange-corrected dielectric functions[1] $\epsilon_{tt}(\kappa, \omega)$ have been used to calculate the pair distribution function[2-4] and correlation energy of an electron gas[2,5,6] and phonon dispersion curves of metals,[7-9] the effect of using exchange-corrected vertex functions $\Lambda_{\vec{k}}(\vec{\kappa}, \omega) = 1/\epsilon_{\vec{k}t}(\vec{\kappa}, \omega)$ on the electron self-energy has not heretofore been calculated. The present calculation of the imaginary part of the self-energy has been stimulated by Kanter's[10] recent measurement of the mean free path (MFP) of electrons 5 eV above the Fermi surface in aluminum. The MFP is inversely proportional to the

imaginary part of the self-energy, and Kanter (at our suggestion) attributed the discrepancy between his measured value and the random-phase-approximation (RPA) theoretical value to the neglect of exchange contributions in[11] ϵ_{RPA}. These arguments were based on the effect of exchange on screening, that is, on the real part of ϵ, whereas the imaginary self-energy depends most strongly on the imaginary part of ϵ and therefore a detailed numerical calculation is required.

It is instructive to compare our use of the exchange-corrected vertex function with the work of Ritchie and Ashley[12] who added a single-exchange scattering diagram screened with ϵ_{RPA} to the MFP calculation. The exchange-corrected vertex function is equivalent to summing this diagram to infinite order, including not only exchange between the incoming electron and an electron from the Fermi sea but also exchange between pairs of electrons within the Fermi sea. Furthermore, self-energy corrections which were neglected by Ritchie and Ashley are included in our vertex function. In the very low-energy limit, the single-exchange scattering diagram of Ritchie and Ashley[12] yields a 70% increase to the RPA MFP in aluminum, whereas the infinite sums included in the present calculation reduce this to a 1% increase (compare the *Kt* and RPA columns of Table II for $K \to 1$).

In Sec. II, a new approximation for $\epsilon_{\vec{k}t}(\vec{\kappa}, \omega)$ is presented. An earlier form[13] of $\epsilon_{\vec{k}t}$ involved an approximation, which although quite acceptable for $\mathrm{Re}\,\epsilon_{\vec{k}t}$, yields obviously incorrect values for $\mathrm{Im}\epsilon_{\vec{k}t}$. In Sec. III, we numerically evaluate the self-energy integral. We compare the $\epsilon_{\vec{k}t}$ results with those obtained from ϵ_{tt} and ϵ_{RPA}. At higher energies, the RPA results differ significantly from Quinn's[14] owing to his analytic approximations and (we presume) insufficient numerical accuracy in his calculations. At 5 eV, there is little difference between the RPA and exchange-corrected results and the discrepancy between theory and experiment is not explained.

II. VERTEX FUNCTION

We have recently derived[13] approximate formulas for $\epsilon_{et}(\kappa, \omega)$, $\epsilon_{\vec{k}t}(\vec{\kappa}, \omega)$, and $\epsilon_{tt}(\kappa, \omega)$, where ϵ_{et} and $\epsilon_{\vec{k}t}$ are the inverse vertex functions of an average electron in the Fermi sea and of a particular electron with wave vector $\vec{k}$ and ϵ_{tt} is the ordinary dielectric function.[1] The basic formula[13] (I5) for ϵ_{et} has independently been derived by Langreth[15] using a variational technique. We estimated the integrals in (I5) with the following sort of approximation:

$$\int_0^{k_F} \left(\frac{1}{E(\vec{k}'-\vec{\kappa}) - E(k') + \omega + i\eta} \; \frac{8\pi}{(\vec{k}-\vec{k}')^2 + K_S^2} \right.$$

$$\left. + \frac{1}{E(\vec{k}'-\vec{\kappa}) - E(k') - \omega - i\eta} \; \frac{8\pi}{(\vec{k}+\vec{\kappa}-\vec{k}')^2 + K_S^2} \right) d^3k'$$

$$\approx \tfrac{1}{2}[A_k \chi(\kappa, \omega) + B_{\vec{k}} \chi^*(\kappa, -\omega)] \quad , \tag{1}$$

where

$$A_k = \frac{1}{2} \frac{\kappa^2}{k^2 + \alpha k_F^2 + K_S^2} \quad , \quad B_{\vec{k}} = \frac{1}{2} \frac{\kappa^2}{(\vec{k}+\vec{\kappa})^2 + \alpha k_F^2 + K_S^2} \quad ,$$

with α a factor between $\frac{1}{2}$ and 1, and

$$\chi(\kappa, \omega) = 4(\pi\kappa)^{-2} \int [E(\vec{k}'-\vec{\kappa}) - E(k') \pm \omega + i\eta]^{-1} d^3k'$$

is given in (I18)–(I21). Having obtained (I13) for ϵ_{et}, Eqs. (I26) and (I31) for $\epsilon_{\vec{k}t}$ and ϵ_{tt} were derived without further approximation.

The approximation (1) consists of replacing $(\vec{k}-\vec{k}')^2$ by $k^2 + \alpha k_F^2$ when $\vec{k}'$ is integrated over the Fermi sea. This is very reasonable for the real part of the integral, but leads to errors in the imaginary part. Take $\omega = 0$ in (1). Then the imaginary part of the integral comes from the pole at $(\vec{k}'-\vec{\kappa})^2 = k'^2$. But with this substitution the second term on the left-hand side becomes the complex conjugate of the first, and the left-hand side is real (for $\omega = 0$). The right-hand side remains complex, however. Because of a further integration over $\vec{k}$ this error cancels out in (I13) and (I31) and ϵ_{et} and ϵ_{tt} are real for $\omega = 0$. On the other hand, the right-hand side of (1) appears explicitly in (I26) for $\epsilon_{\vec{k}t}$. We now replace it with $\frac{1}{4}(A_k + B_{\vec{k}})[\chi(\kappa, \omega) + \chi^*(\kappa, -\omega)]$. For $\omega = 0$, this causes no change in the real part of $\epsilon_{\vec{k}t}$ while causing the imaginary part to vanish. Thus, we have

$$\epsilon_{\vec{k}t}(\vec{\kappa}, \omega) = \frac{\epsilon_{et}(\kappa, \omega)}{\epsilon_{et}(\kappa, \omega) - \frac{1}{2}[\chi(\kappa, \omega) + \chi^*(\kappa, -\omega)][1 - \frac{1}{2}(A_k + B_{\vec{k}})]} \quad . \tag{2}$$

One might argue that although it is not necessary for the reality of $\epsilon_{tt}(\kappa, 0)$ and $\epsilon_{et}(\kappa, 0)$, a similar correction should be made in $\epsilon_{tt}(\kappa, \omega)$ and $\epsilon_{et}(\kappa, \omega)$ for the sake of consistency, i.e.,

$$\{A[\chi^2(\kappa, \omega) + \chi^{*2}(\kappa, -\omega)] + 2B\chi(\kappa, \omega)\chi^*(\kappa, -\omega)\}$$

should be replaced by

$$\tfrac{1}{2}(A+B)[\chi(\kappa, \omega) + \chi^*(\kappa, -\omega)]^2 \quad .$$

This would, however, completely eliminate the exchange matrix element corrections to the plasma frequency which are needed, since it is well known that the infinite-wavelength RPA plasma frequency is exactly correct, to cancel the self-energy corrections to the plasma frequency.

III. NUMERICAL RESULTS

The imaginary part of the self-energy of an electron above the Fermi surface is given by (I39),[13]

$$\Gamma(k) = \pi^{-2} \mathrm{Im} \int d^3q \; \frac{(\vec{q}-\vec{k})^{-2}[1 - f(q)]\theta(k^2 - q^2)}{\epsilon_{\vec{k}t}(\vec{q}-\vec{k}, k^2 - q^2)} \quad , \tag{3}$$

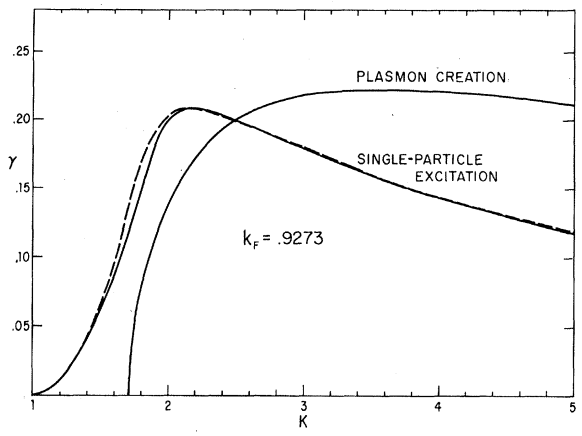

FIG. 1. Normalized imaginary self-energy of a hot electron in aluminum $\gamma = -\Gamma/E_F$ vs normalized wave vector of the hot electron $K = k/k_F$. The solid curves are for the RPA and the broken curve includes exchange corrections.

where $\vec{k}$ is the wave vector of the electron and $\vec{q}$ of the state into which it is being scattered. The factor $1-f(q)$ ensures that the final state lies above the Fermi surface and the step function $\theta(k^2-q^2)$ ensures that it lies below the original state $\vec{k}$. Equation (3) reduces to a two-dimensional numerical integration over μ = the cosine of the angle $\vec{q}$ makes with $\vec{k}$ and over the magnitude of $\vec{q}$. The single-particle excitation contribution (i.e., the $\mathrm{Im}\epsilon_{kt} \neq 0$ contribution) to $\Gamma(k)$ was obtained straightforwardly by dividing the $-1 \leq \mu \leq 1$ and $k_F < q < k$ region into an $N \times M$ mesh. For $k = 1.63k_F$ and less, convergence was obtained with $N = 200$ and $M = 100$ but for $k = 1.75k_F$ and greater, $N = 1600$ or 3200 and $M = 200$ was required.[16] This very slow convergence for $k \geq 1.75k_F$ is due to the region where the plasma line enters the single-particle excitation continuum, i.e., where $\mathrm{Re}\epsilon < \mathrm{Im}\epsilon$. In Fig. 1, $\gamma = -\Gamma/E_F$ is plotted against $K = k/k_F$ for aluminum ($r_s = 2.07$) in the RPA. Comparing the single-particle excitation graph with Quinn's[14] Fig. 2, we see the two curves are similar for very small K, but our curve has a relatively sharp peak of $\gamma = 0.21$ at $K = 2.2$, whereas Quinn's has a very broad peak of $\gamma = 0.14$ at $K = 3.5$. Noting that each point (for $K \geq 1.75$) on the curve took 9 min of CDC 6600 time to calculate, it would not be surprising if Quinn's 1961 calculation failed to converge.

To evaluate Γ_p, the plasma contribution to Γ, we made the following substitutions[17]:

$$Z = |\vec{K} - \vec{Q}| \quad , \quad \Omega = K^2 - Q^2 \quad , \quad U = \Omega/Z \quad , \tag{4}$$

where $\vec{Q} = \vec{q}/k_F$, to obtain

$$\Gamma = \frac{k_F}{\pi K} \iint dU\, dZ\, \mathrm{Im}\, \frac{1}{\epsilon_{kt}(Z, U)} \quad . \tag{5}$$

Using the fact that in the region where ϵ_2 is infinitesmal

$$\mathrm{Im}\frac{1}{\epsilon} = \frac{-\epsilon_2}{\epsilon_1^2 + \epsilon_2^2} = -\pi\delta(\epsilon_1) \quad ,$$

we have

$$\Gamma_p = \frac{-k_F}{K} \int \left(\frac{\partial \epsilon_1}{\partial U}\right)_p^{-1} dZ \quad . \tag{6}$$

From (4) it follows that

$$Z^2 = (K^2 - \Omega_p) - 2K(K^2 - \Omega_p)^{1/2}\mu + K^2 \quad ,$$

or that

$$K - [K^2 - \Omega_p(Z)]^{1/2} \leq Z \leq K + [K^2 - \Omega_p(Z)]^{1/2} \quad , \tag{7}$$

where $\Omega_p(Z) = \omega_p(Z)/k_F^2$. To evaluate (6) with the condition (7), we first determined the plasma line by fixing Z and searching numerically for that value of Ω which made ϵ_1 vanish. This was done for all values of Z between 0.1 and the point where the plasma line enters the single-particle continuum (i.e., $\epsilon_2 \neq 0$) in increments of $\Delta Z = 0.001$. Since this upper limit was less than 0.8 and K is always greater than unity the upper limit of Z (for $r_s = 2.07$) is the end of the plasma line while the lower limit is still given by (7). At the same time that we determined the plasma line, we numerically calculated $(\partial\epsilon_1/\partial U)_p^{-1}$ for each value of Z. The K dependence of Γ_p then enters through the lower limit and through the factor $1/K$. For K^2, only slightly larger than $\Omega_p(Z)$, the lower limit lies above the upper limit and $\Gamma_p = 0$. As K increases, the lower limit continually drops and Γ_p increases rapidly from zero. At large K, the $1/K$ factor dominates and Γ_p slowly decreases. In Fig. 1, we show γ_p as a function of K in the RPA.[18] This curve differs from Quinn's[14] which was obtained analytically with some severe approximations mainly in that it begins at $K \approx 1.725$, whereas, his begins at $K = 1.606$.[19]

In Table I we list $\Omega_p(Z)$ for several values of Z in the RPA and with exchange corrections.[20] The ex-

TABLE I. Normalized plasma frequency $\Omega_p(Z) = \omega_p(Z)/k_F^2$ for several values of $Z = |\vec{k} - \vec{q}|/k_F$ in the RPA and with exchange corrections.

Z	RPA	Exchange
0	1.3530	1.3529
0.100	1.3620	1.3620
0.200	1.3890	1.3862
0.300	1.4356	1.4283
0.400	1.5044	1.4917
0.500	1.6007	1.5829
0.600	1.7339	1.7145
0.700	1.9232	1.9162
0.708	1.9419	1.9385
0.738	2.0208	

TABLE II. Single-particle and plasma contributions to $\gamma = -\Gamma/E_F$ for several values of $K = k/k_F$ evaluated using ϵ_{RPA}, $\epsilon_{\vec{K}t}$, and ϵ_{tt}.

K	RPA		Kt		tt	
1.02	0.000130		0.000129		0.000143	
1.10	0.00311		0.00308		0.00342	
1.20	0.0115		0.0115		0.01281	
1.35	0.0318		0.0323		0.0361	
1.50	0.0624		0.0653		0.0723	
1.63	0.0960		0.1020		0.1122	
1.72		0.0		0.0252		0.0278
1.73		0.0298		0.0345		0.0379
1.74		0.0422		0.0413		0.0453
1.75	0.1296	+0.0499	0.1534	+0.0473	0.1676	+0.0518
2.00	0.1999	+0.1386	0.2026	+0.1266	0.2211	+0.1353
2.25	0.2078	+0.1777	0.2068	+0.1642	0.2249	+0.1737
2.50	0.1999	+0.1990	0.1986	+0.1857	0.2152	+0.1952
3.0	0.1792	+0.2182	0.1802	+0.2059	0.1929	+0.2147
4.0	0.1430	+0.2214	0.1436	+0.2114	0.1513	+0.2186
5.0	0.1176	+0.2115	0.1190	+0.2033	0.1237	+0.2092

change corrected $\Omega_p(0)$ has an error of 0.0001 due to the approximation (1) which causes the cancellation between the exchange matrix element and self-energy contributions to be incomplete. For large Z, the differences between RPA and exchange are much larger than 0.0001 and we believe them to be real. The RPA plasma curve enters the single-particle excitation continuum at $Z = 0.738$, while the exchange curve enters at $Z = 0.708$. This is due partially to the exchange curve lying below the RPA but mainly because the lower boundary of the continuum with exchange is given by $Z^2 + 2Z = \Omega - \Delta$, where Δ is a self-energy correction.[13]

In Table II we list the single-particle and plasma contributions to γ as a function of K obtained with ϵ_{RPA}, $\epsilon_{\vec{K}t}$, and ϵ_{tt}.[21] The RPA plasma contributions are, in general, larger than the Kt and tt because the plasma curve ends at $Z = 0.738$ whereas the Kt and tt end at $Z = 0.708$. On the other hand, because the Kt and tt plasma curve lies below the RPA, their plasma contributions to Γ begin at a slightly smaller value of K. The differences between Kt and tt are due to differences in $(\partial\epsilon_1/\partial U)_\rho$ and have no simple physical interpretation. There is also not much physical interpretation one can give to the differences between the various single-particle contributions. We note that the tt contributions are always greater than the Kt and RPA and that the Kt is mainly larger but can be slightly smaller than the RPA (see Fig. 1). Also the ratio of tt to Kt single-particle contributions decreases steadily towards unity as K increases beyond 1.35. This is to be expected, for the hotter the hot electron is, the less it exchanges with the Fermi sea of electrons and the more like a test particle it becomes (with the exception that the hot electron cannot scatter to states below the Fermi surface).[21]

The lifetime of a hot electron is $\tau = -1/2\Gamma$ and the MFP $\lambda = v\tau$ may be written

$$\lambda = K a_0/\gamma k_F m^* \ , \tag{8}$$

where a_0 is the Bohr radius and m^* is the effective mass of the electron. For $K = 1.1948$, i.e., an electron 5 eV above the Fermi surface, we have $\gamma = 0.0110$ using either ϵ_{RPA} or $\epsilon_{\vec{K}t}$.[22] Assuming $m^* = 1$, this yields $\lambda = 62.0$ Å compared to Kanter's[10] experimental value of 50 Å. The band and electron self-energy contributions to the effective mass are probably quite small. The phonon contribution can also probably be neglected since the 2×10^{-14} sec that the electron spends in a 400-Å film does not give the lattice time to respond. Thus, the discrepancy between the theoretical and experimental MFP must either be attributed to the approximations in $\epsilon_{\vec{K}t}$ or to experimental error. Surface scattering was eliminated from the experimental MFP by considering films of various thicknesses and phonon contributions were removed by subtracting off the temperature-dependent contribution to $1/\lambda$. It was claimed by Kanter that impurity scattering was completely negligible. This claim was based on a very long resistivity MFP measured in the plane of the film. However, it is not obvious that the resistivity in the plane of the film is the same as that perpendicular to the plane. Furthermore, small-angle scattering would not affect the resistivity MFP strongly but would strongly reduce the hot-electron MFP. Therefore, we believe it possible that the electron-electron MFP is somewhat larger than the experimental MFP.

*Research sponsored by the U. S. Air Force Office of Scientific Research Office of Aerospace Research, under Grant No. AFOSR 68-1507.

[1]The subscript tt indicates that ϵ_{tt} is the function that screens the potential produced by a test charge and seen by a second test charge. Similarly $\epsilon_{\vec{k}t}$ screens the potential seen by an electron of wave vector $\vec{k}$ produced by a test charge.

[2]K. S. Singwi, A. Sjolander, M. P. Tosi, and R. H. Land, Phys. Rev. B1, 1044 (1970).

[3]R. W. Shaw, Jr., J. Phys. C 3, 1140 (1970).

[4]P. R. Antoniewicz and L. Kleinman, Phys. Rev. B 2, 2808 (1970).

[5]J. Hubbard, Proc. Roy. Soc. (London) A243, 336 (1957).

[6]P. R. Antoniewicz and L. Kleinman, Phys. Letters 32A, 292 (1970).

[7]L. J. Sham, Proc. Roy. Soc. (London) A283, 33 (1965).

[8]R. W. Shaw, Jr. and R. Pynn, J. Phys. C 2, 2071 (1969).

[9]E. R. Floyd and L. Kleinman, Phys. Rev. B 2, 3947 (1970).

[10]H. Kanter, Phys. Rev. B 1, 522 (1970).

[11]In the RPA, $\epsilon_{\vec{k}t}$ is, of course, identical to ϵ_{tt}.

[12]R. H. Ritchie and J. C. Ashley, J. Phys. Chem. Solids 26, 1689 (1965).

[13]L. Kleinman, Phys. Rev. 172, 383 (1968), hereafter called I.

[14]J. J. Quinn, Phys. Rev. 126, 1453 (1962).

[15]D. C. Langreth, Phys. Rev. 181, 753 (1969), see Eq. (43).

[16]We divided the $M=200$ q integration into four parts each with $M=50$. In one of those four parts $N=3200$ was usually needed for convergence and $N=1600$ was used in the other three.

[17]S. M. Bose, A. Bardasis, A. J. Glick, D. Hone, and P. Longe, Phys. Rev. 155, 379 (1967).

[18]To find the plasma line and evaluate Eq. (6) for 91 different values of K took 14 sec of CDC 6600 time as compared with 9 min to get a single point on the single-particle excitation curve.

[19]We redid the calculation with $r_s=2.0$ to get a more exact comparison with Quinn. Our curve then started at $K\approx 1.715$. Also our maximum value of γ was 0.2125 while Quinn's was 0.195.

[20]The screening constant K_S and the parameter α appearing in Eq. (2) were chosen as in P. R. Antoniewitz and L. Klienman, Phys. Rev. B 2, 2809 (1970), see Eqs. (20) and (21).

[21]The ϵ_{tt} results have no physical meaning and are presented only for the sake of comparison with the ϵ_{RPA} and $\epsilon_{\vec{k}t}$ results. It would be physically meaningful to remove the factor $[1-f(q)]$ from Eq. (3) and then calculate Γ for a test charge (i.e., any particle other than an electron) using ϵ_{tt}.

[22]To one more significant figure $\gamma_{\mathrm{RPA}}=0.01097$ and $\gamma_{Kt}=0.01095$. Note, however, that for some of K the difference is much greater.